RESPONSE FUNCTIONS OF SEMI-LEADED NEUTRON MONITOR COUNT RATES AND LEADER RATES FROM LATITUDE SURVEYS DURING 2019-2020

P. Yakum, S. Khamphakdee, W. Nuntiyakul, D. Ruffolo, P. Evenson, P.-S.Mangeard, A. Sáiz, C. Banglieng, A. Seripienlert, P. Jiang, P. Chuanraksasat, K. Munakata, J. Madsen, B. Soonthornthum, S. Komonjinda

Introduction

We have developed a portable neutron monitor ("Changvan") with three sections to investigate cosmic ray spectral variations via latitude surveys. The Changvan uses the NM64 design for two sections, but the third lacks the lead producer, so we call this a "semi-leaded" neutron monitor. The Changvan was operated on two voyages on the Chinese icebreaker *Xuelong* between Shanghai and Antarctica during 2019 and 2020. Repeated measurements with the same detector over different phases of the solar cycle provide precise information about cosmic ray spectral variation. We report measurements of the response functions of the count rates and leader rates of the unleaded and leaded counters during these two latitude surveys.

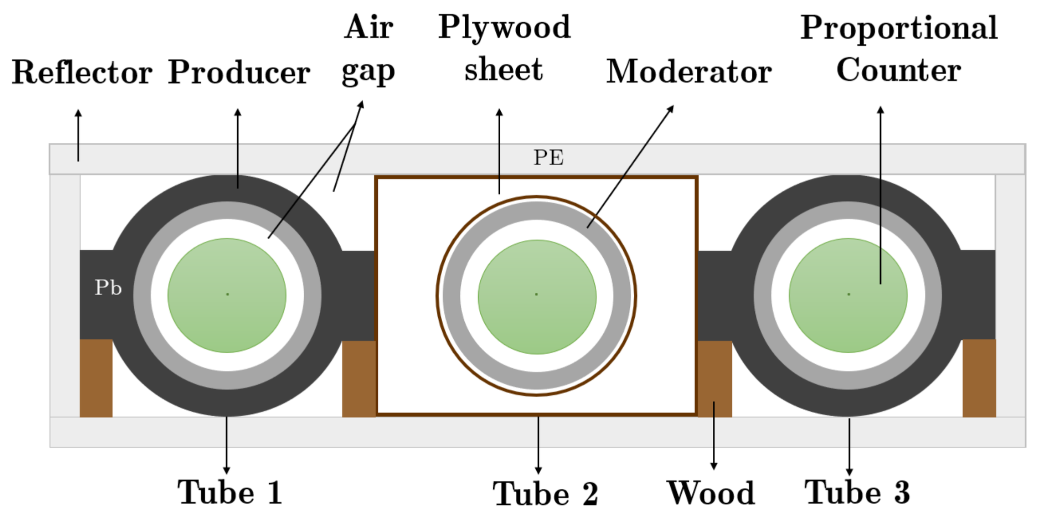

Figure 1: Drawing of the Changvan monitor. Tube 1 and Tube 3 are NM64s. Tube 2 is an unleaded neutron monitor hold onto three supported wooden plates.

Observations

The Changvan was carried by the icebreaker *Xuelong* on research missions conducted by the Polar Research Institute of China (PRIC). The "survey year" refers to the year in which the voyage ended. The Survey year 2019 (CN35) covers the voyage from 2 November 2018 to 11 March 2019, and survey year 2020 (CN36) covers the voyage from 21 October 2019 to 22 April 2020.

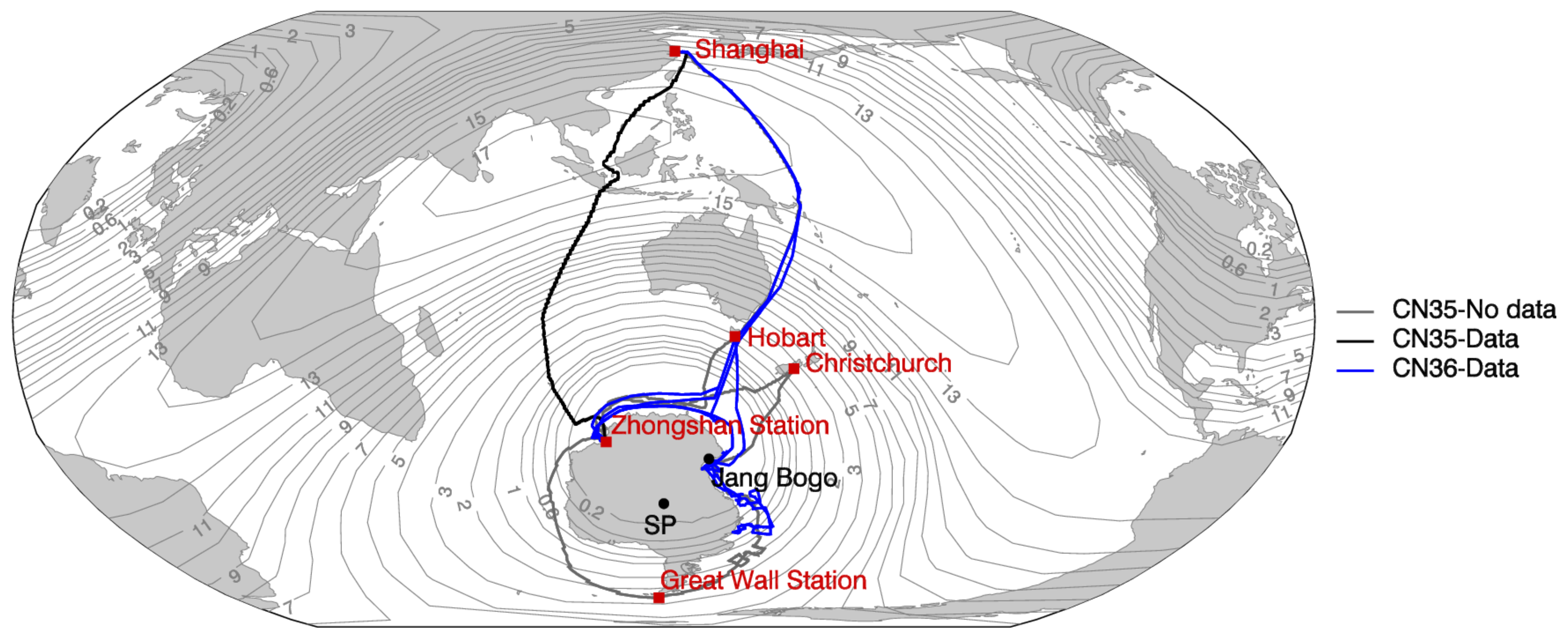

Figure 2: Tracks of the latitude surveys in 2019 and 2020, superimposed on contours of the vertical cutoff rigidity in GV.

Data cleaning

The Changvan records one-second resolution count rate data and hourly time-delay histogram files. The analysis of the count rate data obtained from the ship-borne neutron detectors, we cleaned data based on the one-second distribution and count rate ratios, and then corrected data for barometric pressure by collected data with the same system used in previous surveys [1] .

Analysis of neutron time-delay histograms

We analyze hourly time-delay histograms collected by Changvan neutron monitor during the 2019 and 2020 survey years to calculate the leader fraction (*L*) [2] to remove the effect of chance coincidences of neutrons that did not follow a prior neutron count in the same counter tube due to the same atmospheric secondary particle [3].

Response functions

We used the averaged data between T1 and T3 to find the response functions of the Changvan neutron monitor because T2 has a different configuration. We multiplied leader fraction (*L*) values to the count rate (N) for each cutoff rigidity bin , i.e., 0-1 GV, 1-2 GV,..., 17-18 GV, allowing us to derive what we called "leader rate (*R*)." The *R* supersedes the count rate that removed a chance of coincidence from the same secondary cosmic ray particles in the neutron monitor to avoid problems with multiplicity in a fixed time window. Multiplicity is expected to be dominated by the composition of secondary atmospheric particles and their energy.

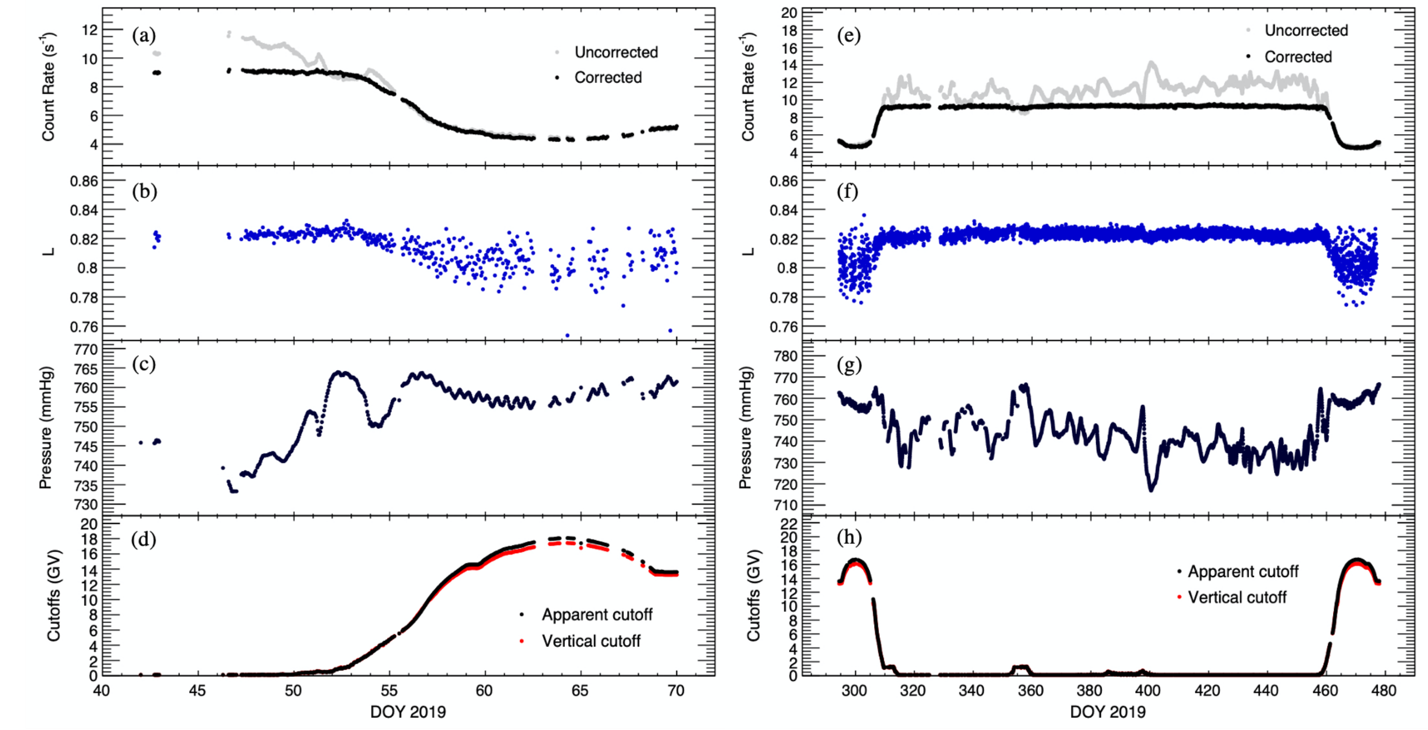

Figure 3: (a)-(d) Data set of the survey year 2019 and (e)-(h) of the survey year 2020, as a function of time. (a) and (e) Hourly averaged count rates for two counter tubes (T1 & T3). (b) and (f) display Leader fraction (*L*). (c) and (g) The barometric pressure was recorded by GPS on the *XueLong* icebreaker. (d) and (h) show geomagnetic cutoff rigidity, where the blackline shows the apparent cutoff rigidity, and the red line shows the vertical cutoff rigidity [4,5,6].

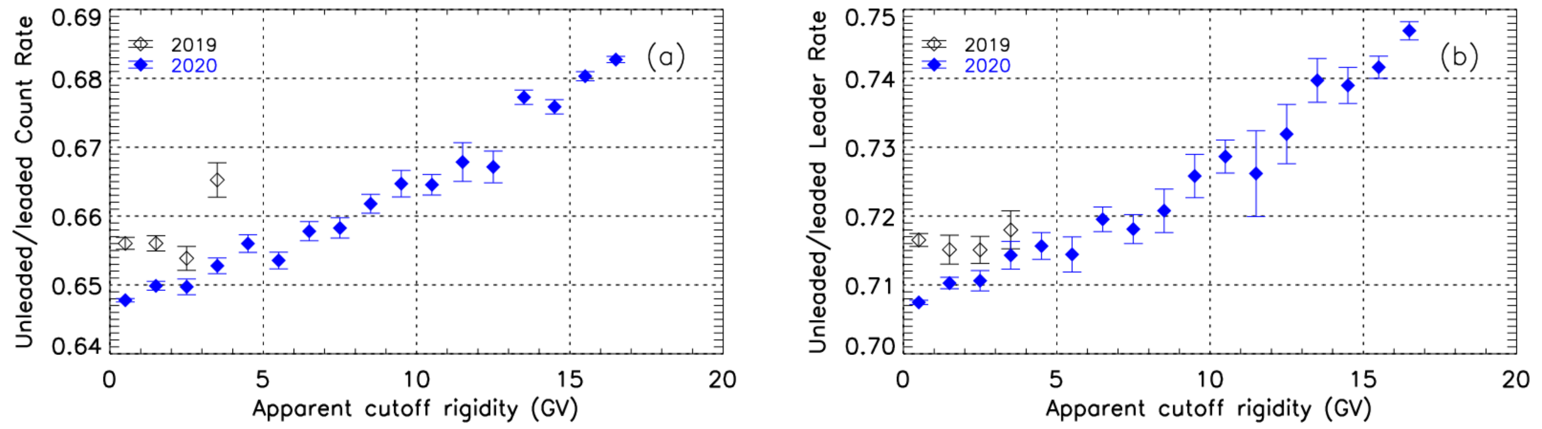

Figure 4: The count rate (left) and leader rate (right) ratio of unleaded vs. leaded counters as a function of apparent cutoff rigidity for the 2019 and 2020 survey years. Here, "unleaded" means T2, and "leaded" means the averaged T1 and T3. Error bars indicate the standard error.

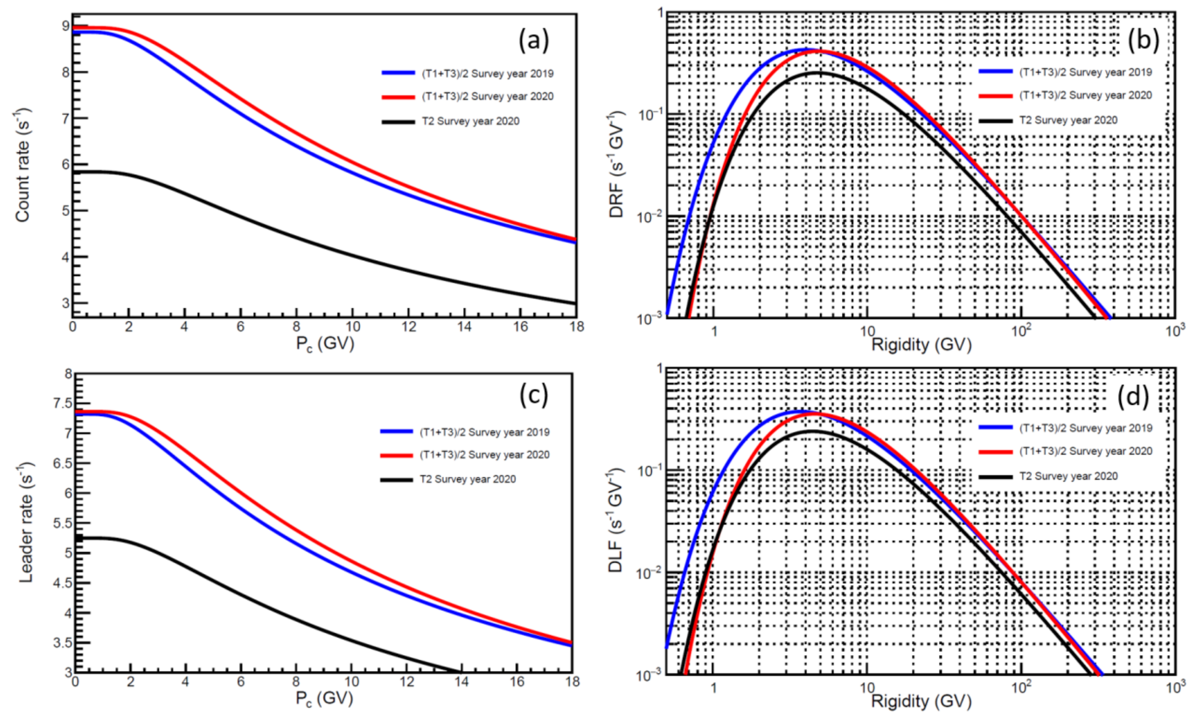

Figure 5: Dorman function fits Vs. Pc for 2019 and 2020 survey years. (a)-(b) Integral and differential count rate response functions. (c)-(d) Integral and differential leader rate response functions.

Conclusion

We have analyzed data and determined the response functions as a function of apparent cutoff rigidity of the count rates and leader rates of the unleaded (T2) and leaded counters (averaged T1& T3) of 2019 and 2020 latitude surveys. In Figure 4, we can see the count rate and leader rate ratio of unleaded vs. leaded counters varies linear trend with geomagnetic cutoff rigidity, indicating sensitivity to the cosmic ray spectrum.

Acknowledgments

The research is supported in part by Thailand Science Research and Innovation via Research Team Promotion Grant RTA6280002. We thank the Northern Science Park (Chiang Mai) for pro-viding laboratory space at the park, which helps the research team working smoothly.

References

[1] Nuntiyakul, W., et al. (2014), Astrophys. J.,795, 11
[2] Yakum, P., et al. (2021), J. Phys.: Conf. Ser., 1719
[3] Ruffolo, D., et al. (2016), Astrophys. J., 817, 38
[4] Bieber, J., J. Clem, P. Evenson et al. (1997), In Proc. of the 25th ICRC, 2, 389–392
[5] Clem, J., J. Bieber, P. Evenson et al. (1997), J. Geophys. Res., 102, 26,919–26,929
[6] Lin, Z., J. Bieber & P. Evenson (1995), J. Geophys. Res., 100, 23,543–23,550